

Exploiting Full/Half-Duplex User Relaying in NOMA Systems

Xinwei Yue, *Student Member, IEEE*, Yuanwei Liu, *Member, IEEE*, Shaoli Kang, Arumugam Nallanathan, *Fellow, IEEE*, and Zhiguo Ding, *Senior Member, IEEE*

Abstract—In this paper, a novel cooperative non-orthogonal multiple access (NOMA) system is proposed, where one near user is employed as decode-and-forward (DF) relaying switching between full-duplex (FD) and half-duplex (HD) mode to help a far user. Two representative cooperative relaying scenarios are investigated insightfully. The *first scenario* is that no direct link exists between the base station (BS) and far user. The *second scenario* is that the direct link exists between the BS and far user. To characterize the performance of potential gains brought by FD NOMA in two considered scenarios, three performance metrics outage probability, ergodic rate and energy efficiency are discussed. More particularly, we derive new closed-form expressions for both exact and asymptotic outage probabilities as well as delay-limited throughput for two NOMA users. Based on the derived results, the diversity orders achieved by users are obtained. We confirm that the use of direct link overcomes zero diversity order of far NOMA user inherent to FD relaying. Additionally, we derive new closed-form expressions for asymptotic ergodic rates. Based on these, the high signal-to-noise radio (SNR) slopes of two users for FD NOMA are obtained. Simulation results demonstrate that: 1) FD NOMA is superior to HD NOMA in terms of outage probability and ergodic sum rate in the low SNR region; and 2) In delay-limited transmission mode, FD NOMA has higher energy efficiency than HD NOMA in the low SNR region; However, in delay-tolerant transmission mode, the system energy efficiency of HD NOMA exceeds FD NOMA in the high SNR region.

Index Terms—Decode-and-forward, full-duplex, half-duplex, non-orthogonal multiple access, user relaying

I. INTRODUCTION

With the rapid increasing demand of wireless networks, the requirements for efficiently exploiting the spectrum is of great significance in new radio (NR) usage scenarios [2]. To achieve higher spectral efficiency of the fifth generation (5G) mobile communication network, non-orthogonal multiple access (NOMA) has received a great deal of attention [3]. Recently, several NOMA schemes have been researched in

This work was supported by National High Technology Research and Development Program of China (863 Program, 2015AA01A709). The work of Z. Ding was supported by the UK EPSRC under grant number EP/L025272/1 and by H2020-MSCA-RISE-2015 under grant number 690750.

X. Yue and S. Kang are with School of Electronic and Information Engineering, Beihang university, Beijing, China. S. Kang is also with State Key Laboratory of Wireless Mobile Communications, China Academy of Telecommunications Technology (CATT), Beijing, China (email: xinwei_yue@buaa.edu.cn, kangshaoli@catt.cn).

Y. Liu and A. Nallanathan are with School of Electronic Engineering and Computer Science, Queen Mary University of London, London, UK (email: {yuanwei.liu, arumugam.nallanathan}@qcl.ac.uk).

Z. Ding is with the Department of Electrical Engineering, Princeton University, Princeton, USA and also with the School of Computing and Communications, Lancaster University, U.K (e-mail: z.ding@lancaster.ac.uk). Part of this work has been submitted to IEEE ICC 2017 [1].

detail, such as power domain NOMA (PD-NOMA) [4], sparse code multiple access (SCMA) [5], pattern division multiple access (PDMA) [6], multiuser sharing access (MUSA) [7], etc. Generally speaking, NOMA schemes can be classified into two categories, namely power-domain NOMA¹ and code-domain NOMA. Downlink multiuser superposition transmission (DL MUST), the special case of NOMA, has been studied for 3rd generation partnership project (3GPP) in [8]. The pivotal characteristic of NOMA is to allow multiple users to share the same physical resource (i.e., time/frequency/code) via different power levels. At the receiver side, the successive interference cancellation (SIC) is carried out [9].

So far, point-to-point NOMA has been studied extensively in [10–14]. To evaluate the performance of uplink NOMA systems, the authors in [10] proposed the uplink NOMA transmission scheme to achieve higher system rate. The expressions of outage probability and achievable sum rates for uplink NOMA were derived with a novel uplink control protocol in [11]. Regarding downlink NOMA scenarios, authors in [12] analyzed the outage behavior and ergodic rates of NOMA networks, where multiple NOMA users are spatially randomly deployed in a disc. In [13], the cognitive radio inspired NOMA concept was proposed, in which the influence of user pairing with the fixed power allocation in NOMA systems was discussed. As the interplay between NOMA and cognitive radio is bidirectional, NOMA was also applied to cognitive radio networks in [14]. More particularly, the analytical expressions of outage probability were derived and diversity orders were characterized. Apart from the above works, a new opportunistic NOMA scheme was proposed in [15] to improve the efficiency of SIC. In [16], the flexible power allocation mode was researched in terms of outage probability for hybrid NOMA systems. The quantum-assisted multiple users transmission mode for NOMA was proposed in [17], which utilizes the minimum bit error ratio criterion to optimize the predefined transmitted information. The author of [18] has studied the linear MUST scheme for NOMA to maximize sum rate of the entire network. With the emphasis on physical layer security, in [19], authors have adopted two effective approaches, namely protected zone and artificial noise for enhancing the secrecy performance of NOMA networks with the aid of stochastic geometry.

Cooperative communication is a particularly effective approach by providing the higher diversity as well as extending

¹In this paper, we focus on power-domain NOMA and use NOMA to represent PD-NOMA.

the coverage of networks [20]. Current NOMA research contributions in terms of cooperative communication mainly include two aspects. The *first aspect* is the application of NOMA into cooperative networks [21–24]. The coordinated two-point system with superposition coding (SC) was researched in the downlink communication in [21]. The authors in [22, 23] investigated outage probability and system capacity of decode-and-forward (DF) relaying for NOMA. In [24], the outage behavior of amplify-and-forward (AF) relaying with NOMA has been discussed over Nakagami- m fading channels. The *second aspect* is cooperative NOMA, which was first proposed in [25]. The key idea of cooperative NOMA is to regard the near NOMA user as a DF user relaying to help far NOMA user. On the standpoint of considering energy efficiency issues, simultaneous wireless information and power transfer (SWIPT) was employed at the near NOMA user, which was regarded as DF relaying in [26].

Although cooperative NOMA is capable of enhancing the performance gains for far user, it results in additional bandwidth costs for the system. To avoid this issue, one promising solution is to adopt the full-duplex (FD) relay technology. FD relay receives and transmits simultaneously in the same frequency band, which is the reason why it has attracted significant interest to realize more spectrally efficient systems [27]. In a general case, due to the imperfect isolation or cancellation process, FD operation may suffer from residual loop self-interference (LI) which is modeled as a fading channel. With the development of signal processing and antenna technologies, relaying with FD operation is feasible [28]. Recently, FD relay technologies have been proposed as a promising technique for 5G networks in [29]. Two main types of FD relay techniques, namely FD AF relaying and FD DF relaying, have been discussed in [30–32]. The expressions for outage probability of FD AF relaying were provided in [30], which considers the processing delay of relaying in practical scenarios. In [31], the performance of FD AF relaying in terms of outage probability was investigated considering the direct link. The authors in [32] characterized the outage performance of FD DF relaying. It is demonstrated that the optimal duplex mode can be selected according to the outage probability. Furthermore, the operations of randomly switching between FD and HD mode were considered for enhancing spectral efficiency in [33].

A. Motivations and Related Works

While the aforementioned research contributions have laid a solid foundation with providing a good understanding of cooperative NOMA and FD relay technology, the treatises for investigating the potential benefits by integrating these two promising technologies are still in their infancy. Some related cooperative NOMA studies have been investigated in [25, 34]. In [25], it is demonstrated that the maximum diversity order can be obtained for all users, but cooperative NOMA with a direct link was only considered with HD operation mode. In [34], the authors investigated the performance of FD device-to-device based cooperative NOMA. However, only the outage performance of far user was analyzed. To the best

of our knowledge, there is no existing work investigating the impact of the direct link for FD user relaying on the network performance, which motivates us to develop this treatise. Also, there is lack of systematic performance evaluation metrics i.e., considering ergodic rate and energy efficiency in terms of FD/HD NOMA systems. Different from [25, 34], we present a comprehensive investigation on adopting near user as a FD/HD relaying to improve the reliability of far user. More specifically, we attempt to explore the potential ability of user relaying in NOMA networks with identifying the following key impact factors.

- Will FD NOMA relaying bring performance gains compared to HD NOMA relaying? If yes, what is the condition?
- What is the impact of direct link on the considered system? Will it significantly improve the network performance in terms of outage probability and throughput?
- Will NOMA relaying bring performance gains compared to conventional orthogonal multiple access (OMA) relaying?
- In delay-limited/tolerant transmission modes, what are the relationships between energy efficiency (EE) and HD/FD NOMA systems?

B. Contributions

In this paper, we propose a comprehensive NOMA user relaying system, where near user can switch between FD and HD mode according to the channel conditions. We also consider the setting of two scenarios in which the direct link exists or not between the BS and far user. Based on our proposed NOMA user relaying systems, the primary contributions of this paper are summarised as follows:

- 1) *Without direct link*: We derive the closed-form expressions of outage probability for the near user and far user, respectively. For obtaining more insights, we further derive the asymptotic outage probability of two users and obtain diversity orders at high SNR. We demonstrate that FD NOMA converges to an error floor and results in a zero diversity order. We show that FD NOMA is superior to HD NOMA in terms of outage probability in the low SNR region rather than in the high SNR region. In addition, we also obtain the diversity orders of two users for HD NOMA. Furthermore, we analyze the system throughput in delay-limited transmission according to the derived outage probability.
- 2) *Without direct link*: We study the ergodic rate of two users for FD/HD NOMA. To gain better insights, we derive the asymptotic ergodic rates of two users and obtain the high SNR slopes. We demonstrate that the ergodic rate of far user converges to a throughput ceiling for FD/HD NOMA in the high SNR region. Moreover, we also demonstrate that FD NOMA outperforms HD NOMA in terms of ergodic sum rate in the low SNR region.
- 3) *With direct link*: We first derive the closed-form expression in terms of outage probability for far user. In order to get the corresponding diversity order, we also derive

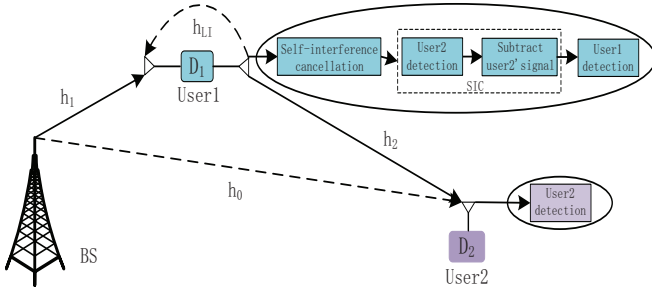


Fig. 1: A downlink FD/HD cooperative NOMA system model.

the approximated outage probability of far user. We find that the reliability of far user is improved with the help of direct link. We confirm that the use of direct link overcomes the zero diversity order of far user inherent to conventional FD relaying. For the near user, the diversity order is the same as that of FD relaying. Additionally, we conclude that the superiority of FD NOMA is no longer apparent with the values of LI increasing.

- 4) *With direct link*: We analyze the ergodic rate of far user for FD/HD NOMA. For this scenario, it is the fact that the ergodic rate of near user is invariant which is not affected by the direct link. Similarly, we also derive the approximated expressions for ergodic rate and obtain the high SNR slopes. We demonstrate that the use of direct link is incapable of assisting far user to obtain additional high SNR slope.
- 5) *Energy efficiency*: We derive expressions in terms of energy efficiency for FD/HD NOMA. We conclude that FD NOMA without/with direct link have a higher energy efficiency corresponding to HD NOMA in the low SNR region for delay-limited transmission mode. However, in delay-tolerant transmission mode, the system energy efficiency of HD NOMA exceeds FD NOMA without/with direct link.

C. Organization and Notation

The rest of the paper is organized as follows. In Section II, the system model of user relaying for FD NOMA is set up. In Section III, the analytical expressions for outage probability, diversity order and throughput of FD/HD user relaying are derived and analyzed. In Section IV, the performance of user relaying for FD/HD NOMA are evaluated in terms of ergodic rate. Section V considers the system energy efficiency for FD/HD NOMA systems. Analytical results and simulations are presented in Section VI. Section VII concludes the paper.

The main notations of this paper is shown as follows: $\mathbb{E}\{\cdot\}$ denotes expectation operation; $f_X(\cdot)$ and $F_X(\cdot)$ denote the probability density function (PDF) and the cumulative distribution function (CDF) of a random variable X ; \propto represents “be proportional to”.

II. SYSTEM MODEL

We consider a FD cooperative NOMA system consisting of one source, i.e., the BS, that intends to communicate with far

user D_2 via the assistance of near user D_1 illustrated in Fig. 1. D_1 is regarded as user relaying and DF protocol is employed to decode and forward the information to D_2 . To enable FD communication, D_1 is equipped with one transmit antenna and one receive antenna, while the BS and D_2 are single-antenna nodes. Note that D_1 can switch operation between FD and HD mode. All wireless links in network are assumed to be independent non-selective block Rayleigh fading and are disturbed by additive white Gaussian noise with mean power N_0 . h_1 , h_2 , and h_0 are denoted as the complex channel coefficient of $BS \rightarrow D_1$, $D_1 \rightarrow D_2$, and $BS \rightarrow D_2$ links, respectively. The channel power gains $|h_1|^2$, $|h_2|^2$ and $|h_0|^2$ are assumed to be exponentially distributed random variables (RVs) with the parameters Ω_i , $i \in \{1, 2, 0\}$, respectively. When D_1 operates in FD mode, we assume that an imperfect self-interference cancellation scheme² is executed at D_1 such as in [31, 35]. The LI is modeled as a Rayleigh fading channel with coefficient h_{LI} , and Ω_{LI} is the corresponding average power. To analyze HD NOMA, we introduce the switching operation factor detailed in the following.

During the k -th time slot, according to [12], D_1 receives the superposed signal and loop interference signal simultaneously. The observation at D_1 is given by

$$y_{D_1}[k] = h_1(\sqrt{a_1 P_s} x_1[k] + \sqrt{a_2 P_s} x_2[k]) + h_{LI} \sqrt{\varpi P_r} x_{LI}[k - \tau] + n_{D_1}[k], \quad (1)$$

where ϖ is the switching operation factor between FD and HD mode. $\varpi = 1$ and $\varpi = 0$ denote D_1 working in FD and HD mode, respectively. Based on the practical application scenarios, we can select the different operation mode. $x_{LI}[k - \tau]$ denotes loop interference signal and τ denotes the processing delay at D_1 with an integer $\tau \geq 1$. More particularly, we assume that the time k satisfies the relationship $k \geq \tau$. P_s and P_r are the normalized transmission powers at the BS and D_1 , respectively. x_1 and x_2 are the signals for D_1 and D_2 , respectively. a_1 and a_2 are the corresponding power allocation coefficients. To stipulate better fairness between the users, we assume that $a_2 > a_1$ with $a_1 + a_2 = 1$. The SIC³ [36] can be invoked by D_1 for first detecting D_2 having a larger transmit power, which has less inference signal. Then the signal of D_2 can be detected from the superposed signal. Therefore, the received signal-to-interference-plus-noise ratio (SINR) at D_1 to detect D_2 's message x_2 is given by

$$\gamma_{D_2 \rightarrow D_1} = \frac{|h_1|^2 a_2 \rho}{|h_1|^2 a_1 \rho + \varpi |h_{LI}|^2 \rho + 1}, \quad (2)$$

where $\rho = \frac{P_s}{N_0}$ is the transmit signal-to-noise ratio (SNR). Note that x_1 and x_2 are supposed to be normalized unity power signals, i.e., $\mathbb{E}\{x_1^2\} = \mathbb{E}\{x_2^2\} = 1$.

²LI refers to the signals that are transmitted by a FD relaying and looped back to the receiver simultaneously. Through radio frequency (RF) cancellation, antenna cancellation and signal process technologies, etc, those LI can be suppressed to a lower level. However, LI still remains in the receiver due to imperfect self-interference cancellation, when decoding the desired signal.

³It is assumed that perfect SIC is employed at D_1 , our future work will relax this ideal assumption.

After SIC, the received SINR at D_1 to detect its own message x_1 is given by

$$\gamma_{D_1} = \frac{|h_1|^2 a_1 \rho}{\varpi |h_{LI}|^2 \rho + 1}. \quad (3)$$

In the FD mode, the received signal at D_2 is written as $y_{D_2}[k] = h_0(\sqrt{a_1 P_s} x_1[k] + \sqrt{a_2 P_s} x_2[k]) + h_2 \sqrt{P_r} x_2[k - \tau] + n_{D_2}[k]$. However, the observation at D_2 for the direct link is written as $y_{1,D_2}[k] = h_0(\sqrt{a_1 P_s} x_1[k] + \sqrt{a_2 P_s} x_2[k]) + n_{D_2}[k]$. Due to the existence of residue interference (RI) from relaying link, the received SINR at D_2 to detect x_2 for direct link is given by

$$\gamma_{1,D_2}^{RI} = \frac{|h_0|^2 a_2 \rho}{|h_0|^2 a_1 \rho + \kappa |h_2|^2 \rho + 1}, \quad (4)$$

where κ denotes the impact levels of RI. Since DF relaying protocol is invoked in D_1 , we assume that D_1 can decode and forward the signal x_2 to D_2 successfully for relaying link from D_1 to D_2 . As a consequence, the observation at D_2 for relaying link is written as $y_{2,D_2}[k] = h_2 \sqrt{P_r} x_2[k - \tau] + n_{D_2}[k]$. Similarly, considering the impact of RI from direct link, the received SINR at D_2 to x_2 for relaying link is given by

$$\gamma_{2,D_2}^{RI} = \frac{|h_2|^2 \rho}{\kappa |h_0|^2 \rho + 1}. \quad (5)$$

As stated in [31,33], the relaying link corresponding to direct link from BS to D_2 has small time delay for any transmitted signals. In other words, there is some temporal separation between the signal from D_1 and BS. To derive the theoretical results for practical NOMA systems, we assume that these signals from D_1 and BS are fully resolvable by D_2 [34]. Hence, we provide the upper bounds of (4) and (5) in the following parts, which are the received SINRs at D_2 to detect x_2 for direct link and relaying link, i.e.

$$\gamma_{1,D_2} = \frac{|h_0|^2 a_2 \rho}{|h_0|^2 a_1 \rho + 1}, \quad (6)$$

and

$$\gamma_{2,D_2} = |h_2|^2 \rho, \quad (7)$$

respectively. At this moment, the signals from the relaying link and direct link are combined by maximal ratio combining (MRC) at D_2 . So the received SINR after MRC at D_2 is given by

$$\gamma_{D_2}^{MRC} = |h_2|^2 \rho + \frac{|h_0|^2 a_2 \rho}{|h_0|^2 a_1 \rho + 1}. \quad (8)$$

III. OUTAGE PROBABILITY

When the target rate of users is determined by its quality of service (QoS), the outage probability is an important metric for performance evaluation. We will evaluate the outage performance in two representative scenarios in the following.

A. User Relaying without Direct Link

In this subsection, the first scenario is investigated in terms of outage probability.

1) *Outage Probability of D_1* : According to NOMA protocol, the complementary events of outage at D_1 can be explained as: D_1 can detect x_2 as well as its own message x_1 . From the above description, the outage probability of D_1 is expressed as

$$P_{D_1}^{FD} = 1 - \text{Pr}(\gamma_{D_2 \rightarrow D_1} > \gamma_{th_2}^{FD}, \gamma_{D_1} > \gamma_{th_1}^{FD}), \quad (9)$$

where $\varpi = 1$. $\gamma_{th_1}^{FD} = 2^{R_1} - 1$ with R_1 being the target rate at D_1 to detect x_1 and $\gamma_{th_2}^{FD} = 2^{R_2} - 1$ with R_2 being the target rate at D_1 to detect x_2 .

The following theorem provides the outage probability of D_1 for FD NOMA.

Theorem 1. *The closed-form expression for the outage probability of D_1 is given by*

$$P_{D_1}^{FD} = 1 - \frac{\Omega_1}{\Omega_1 + \rho \varpi \theta_1 \Omega_{LI}} e^{-\frac{\theta_1}{\Omega_1}}, \quad (10)$$

where $\varpi = 1$. $\theta_1 = \max(\tau_1, \beta_1)$, $\tau_1 = \frac{\gamma_{th_2}^{FD}}{\rho(a_2 - a_1 \gamma_{th_2}^{FD})}$ and $\beta_1 = \frac{\gamma_{th_1}^{FD}}{a_1 \rho}$. Note (10) is derived on the condition of $a_2 > a_1 \gamma_{th_2}^{FD}$.

Proof: By definition, J_1 denotes the complementary event at D_1 and is calculated as

$$\begin{aligned} J_1 &= \text{Pr}\left(|h_1|^2 \geq (\varpi |h_{LI}|^2 \rho + 1) \theta_1\right) \\ &= \int_0^\infty \int_{(x\varpi\rho+1)\theta_1}^\infty f_{|h_{LI}|^2}(x) f_{|h_1|^2}(y) dx dy \\ &= \frac{\Omega_1}{\Omega_1 + \rho \varpi \theta_1 \Omega_{LI}} e^{-\frac{\theta_1}{\Omega_1}}. \end{aligned} \quad (11)$$

Substituting (11) into (9), (10) can be obtained and the proof is completed. ■

Corollary 1. *Based on (10), the outage probability of D_1 for HD NOMA with $\varpi = 0$ is given by*

$$P_{D_1}^{HD} = 1 - e^{-\frac{\theta_2}{\Omega_1}}, \quad (12)$$

where $\gamma_{th_1}^{HD} = 2^{2R_1-1}$ and $\gamma_{th_2}^{HD} = 2^{2R_2-1}$ denote the target SNRs at D_1 to detect x_1 and x_2 with HD mode, respectively. $\theta_2 = \max(\tau_2, \beta_2)$, $\beta_2 = \frac{\gamma_{th_1}^{HD}}{a_1 \rho}$ and $\tau_2 = \frac{\gamma_{th_2}^{HD}}{\rho(a_2 - a_1 \gamma_{th_2}^{HD})}$ with $a_2 > a_1 \gamma_{th_2}^{HD}$.

2) *Outage Probability of D_2* : The outage events of D_2 can be explained as below. The first is that D_1 cannot detect x_2 . The second is that D_2 cannot detect its own message x_2 on the conditions that D_1 can detect x_2 successfully. Based on these, the outage probability of D_2 is expressed as

$$\begin{aligned} P_{D_2, nodir}^{FD} &= \text{Pr}(\gamma_{D_2 \rightarrow D_1} < \gamma_{th_2}^{FD}) \\ &+ \text{Pr}(\gamma_{2,D_2} < \gamma_{th_2}^{FD}, \gamma_{D_2 \rightarrow D_1} > \gamma_{th_2}^{FD}), \end{aligned} \quad (13)$$

where $\varpi = 1$.

The following theorem provides the outage probability of D_2 for FD NOMA.

Theorem 2. The closed-form expression for the outage probability of D_2 without direct link is given by

$$P_{D_2, \text{nodir}}^{FD} = 1 - \frac{\Omega_1}{\Omega_1 + \rho \varpi \tau_1 \Omega_{LI}} e^{-\left(\frac{\tau_1}{\Omega_1} + \frac{\gamma_{th2}^{FD}}{\rho \Omega_2}\right)}, \quad (14)$$

where $\varpi = 1$.

Proof: By definition, J_2 and J_3 denote the first and second outage events, respectively. The process calculated is given by

$$\begin{aligned} J_2 &= \Pr\left(|h_1|^2 < \tau_1 \left(\varpi |h_{LI}|^2 \rho + 1\right)\right) \\ &= \int_0^\infty \int_0^{\tau_1(\varpi y \rho + 1)} f_{|h_1|^2}(x) f_{|h_{LI}|^2}(y) dx dy \\ &= 1 - \frac{\Omega_1}{\Omega_1 + \rho \varpi \tau_1 \Omega_{LI}} e^{-\frac{\tau_1}{\Omega_1}}. \end{aligned} \quad (15)$$

Applying some algebraic manipulations, J_3 is given by:

$$J_3 = \frac{\Omega_1}{\Omega_1 + \rho \varpi \tau_1 \Omega_{LI}} e^{-\frac{\tau_1}{\Omega_1}} \left(1 - e^{-\frac{\gamma_{th2}^{FD}}{\rho \Omega_2}}\right). \quad (16)$$

Combining (15) and (16), (14) can be obtained and the proof is completed. ■

Corollary 2. Based on (14), the outage probability of D_2 without direct link for HD NOMA with $\varpi = 0$ is given by

$$P_{D_2, \text{nodir}}^{HD} = 1 - e^{-\frac{\tau_2}{\Omega_1} - \frac{\gamma_{th2}^{HD}}{\rho \Omega_2}}. \quad (17)$$

3) *Diversity Analysis:* To get more insights, the asymptotic diversity analysis is provided in terms of outage probability investigated in high SNR region. The diversity order is defined as

$$d = - \lim_{\rho \rightarrow \infty} \frac{\log(P_D^\infty(\rho))}{\log \rho}. \quad (18)$$

a) D_1 for FD NOMA case: Based on analytical result in (10), when $\rho \rightarrow \infty$, the asymptotic outage probability of D_1 for FD NOMA with $e^{-x} \approx 1 - x$ is given by

$$P_{D_1}^{FD, \infty} = 1 - \frac{\Omega_1}{\Omega_1 + \rho \theta_1 \Omega_{LI}}. \quad (19)$$

Substituting (19) into (18), we can obtain $d_{D_1}^{FD} = 0$.

Remark 1. The diversity order of D_1 is zero, which is the same as the conventional FD relaying.

b) D_1 for HD NOMA case: Based on analytical result in (12), the asymptotic outage probability of D_1 for HD NOMA is given by

$$P_{D_1}^{HD, \infty} = \frac{\theta_2}{\Omega_1} \propto \frac{1}{\rho}. \quad (20)$$

Substituting (20) into (18), we can obtain $d_{D_1}^{HD} = 1$.

c) D_2 for FD NOMA case: Based on (14), the asymptotic outage probability of D_2 for FD NOMA is given by

$$P_{D_2, \text{nodir}}^{FD, \infty} = 1 - \frac{\Omega_1 \Omega_2 \rho - \Omega_1 \gamma_{th2}^{FD} - \tau_1 \rho \Omega_2}{\Omega_2 \rho (\Omega_1 + \tau_1 \rho \Omega_{LI})}. \quad (21)$$

Substituting (21) into (18), we can obtain $d_{D_2, \text{nodir}}^{FD} = 0$.

Remark 2. The diversity order of D_2 is zero, which is the same as D_1 in FD NOMA.

d) D_2 for HD NOMA case: Based on (17), the asymptotic outage probability of D_2 for HD NOMA is given by

$$P_{D_2, \text{nodir}}^{HD, \infty} = \frac{\gamma_{th2}^{HD}}{\rho \Omega_2} + \frac{\tau_2}{\Omega_1} \propto \frac{1}{\rho}. \quad (22)$$

Substituting (22) into (18), we can obtain $d_{D_2, \text{nodir}}^{HD} = 1$.

Remark 3. As can be observed that $P_{D_1}^{FD, \infty}$ and $P_{D_2, \text{nodir}}^{FD, \infty}$ are a constant independent of ρ , respectively. Substituting (19) and (21) into (18), we see that there are the error floors for outage probability of two users.

4) *Throughput Analysis:* In this subsection, the delay-limited transmission mode [26, 37] is considered for FD/HD NOMA.

a) *FD NOMA case:* In this mode, the BS transmits information at a constant rate R , which is subject to the effect of outage probability due to wireless fading channels. The system throughput of FD NOMA without direct link is given by

$$R_{l, \text{nodir}}^{FD} = (1 - P_{D_1}^{FD}) R_1 + (1 - P_{D_2, \text{nodir}}^{FD}) R_2, \quad (23)$$

where $P_{D_1}^{FD}$ and $P_{D_2, \text{nodir}}^{FD}$ are given in (10) and (14), respectively.

b) *HD NOMA case:* Similar to (23), the system throughput of HD NOMA without direct link is given by

$$R_{l, \text{nodir}}^{HD} = (1 - P_{D_1}^{HD}) R_1 + (1 - P_{D_2, \text{nodir}}^{HD}) R_2, \quad (24)$$

where $P_{D_1}^{HD}$ and $P_{D_2, \text{nodir}}^{HD}$ are given in (12) and (17), respectively.

B. User Relaying with Direct Link

In this subsection, we explore a more challenging scenario, where the direct link between the BS and D_2 is used to convey information and system reliability can be improved. However, the outage probability of D_1 will not be affected by the direct link. As such, we only show outage probability of D_2 in the following.

1) *Outage Probability of D_2 :* For the second scenario, the outage events of D_2 for FD NOMA is described as below. One of the events is when x_2 can be detected at D_1 , but the received SINR after MRC at D_2 in one slot is less than its target SNR. Another event is that neither D_1 nor D_2 can detect x_2 . Therefore, the outage probability of D_2 is expressed as

$$\begin{aligned} P_{D_2, \text{dir}}^{FD, RI} &= \Pr\left(\gamma_{1, D_2}^{RI} + \gamma_{2, D_2}^{RI} < \gamma_{th2}^{FD}, \gamma_{D_2 \rightarrow D_1} > \gamma_{th2}^{FD}\right) \\ &\quad + \Pr\left(\gamma_{D_2 \rightarrow D_1} < \gamma_{th2}^{FD}, \gamma_{1, D_2} < \gamma_{th2}^{FD}\right). \end{aligned} \quad (25)$$

Unfortunately, the closed-form expression of (25) for D_2 can not be derived successfully. However, it can be evaluated by using numerical simulations. To further obtain a theoretical result for D_2 , exploiting the upper bounds of received SINRs derived in (6) and (7), the outage probability of D_2 is expressed as

$$\begin{aligned} P_{D_2, \text{dir}}^{FD} &= \Pr\left(\gamma_{D_2}^{MRC} < \gamma_{th2}^{FD}, \gamma_{D_2 \rightarrow D_1} > \gamma_{th2}^{FD}\right) \\ &\quad + \Pr\left(\gamma_{D_2 \rightarrow D_1} < \gamma_{th2}^{FD}, \gamma_{1, D_2} < \gamma_{th2}^{FD}\right), \end{aligned} \quad (26)$$

where $\varpi = 1$.

The following theorem provides the outage probability of D_2 for FD NOMA.

Theorem 3. *The closed-form expression for the outage probability of D_2 with direct link is given by*

$$P_{D_2,dir}^{FD} = \left\{ 1 - e^{-\frac{\tau_1}{\Omega_0}} - \sum_{n=0}^{\infty} \frac{(-1)^n e^\varphi}{n! \phi_2^{n+1}} \left[\frac{(-1)^{2n+1} \phi_1^{n+1}}{(n+1)!} \right. \right. \\ \left. \left. \times (\text{Ei}(\psi) - \text{Ei}(\phi_1)) + \sum_{k=0}^n \frac{(1 + a_1 \rho \tau_1)^{n+1} e^\psi \psi^k - e^{\phi_1} \phi_1^k}{(n+1)n \cdots (n+1-k)} \right] \right\} \\ \times \chi e^{-\frac{\tau_1}{\Omega_1}} + \left[\left(1 - \chi e^{-\frac{\tau_1}{\Omega_1}} \right) \left(1 - e^{-\frac{\tau_1}{\Omega_0}} \right) \right], \quad (27)$$

where $\varphi = \frac{1}{\rho a_1 \Omega_0} - \frac{\gamma_{th_2}^{FD}}{\rho \Omega_2} - \phi_1$, $\phi_1 = \frac{-a_2}{a_1 \rho \Omega_2}$, $\phi_2 = a_1 \rho \Omega_0$, $\psi = \frac{-a_2}{a_1 \rho \Omega_2 (1 + a_1 \rho \tau_1)}$ and $\chi = \frac{\Omega_1}{\Omega_1 + \tau_1 \rho \Omega_{LI}}$. $\text{Ei}(\cdot)$ is the exponential integral function [38, Eq. (8.211.1)].

Proof: See Appendix A. ■

2) *Diversity Analysis:* In this subsection, the diversity order of D_2 with direct link for FD NOMA is analyzed in the following.

a) *D_2 for FD NOMA case:* For D_2 with direct link, it is challenging to obtain diversity order from (27). We can use Gaussian-Chebyshev quadrature to find an approximation from (26) and the approximated expression of outage probability for D_2 at high SNR is given by

$$P_{D_2,dir}^{FD,appro} = \left[\frac{\tau_1}{\Omega_0} - \left(1 - \frac{\Omega_2 \tau_1 + 2\Omega_0 \tau_1 (a_2 - a_1 \gamma_{th_2}^{FD})}{2\Omega_0 \Omega_2} \right) \right] \\ \times \frac{\tau_1 \pi}{2N \Omega_0} \sum_{n=1}^N \left(1 + \frac{(s_n + 1) \tau_1 a_2}{\Omega_2 ((s_n + 1) \tau_1 a_1 \rho + 2)} - \frac{s_n \tau_1}{2\Omega_0} \right) \\ \times \sqrt{1 - s_n^2} \left[\frac{\Omega_1}{(\Omega_1 + \tau_1 \rho \Omega_{LI})} + \left(1 - \frac{\Omega_1}{(\Omega_1 + \tau_1 \rho \Omega_{LI})} \right) \frac{\tau_1}{\Omega_0} \right], \quad (28)$$

where N is a parameter to ensure a complexity-accuracy tradeoff, $s_n = \cos\left(\frac{2n-1}{2N}\pi\right)$. Substituting (28) into (18), we can obtain $d_{D_2,dir}^{FD} = 1$.

Remark 4. *From above explanation, the observation is that the direct link ($BS \rightarrow D_2$) to convey information is an effective way to overcome the problem of zero diversity order for D_2 .*

b) *D_2 for HD NOMA case:* The outage performance of D_2 for HD NOMA has been investigated in [25] and we can obtain $d_{D_2,dir}^{HD} = 2$.

3) *Throughput Analysis:* Based on the derived results of outage probability above, we obtain the throughput expressions for FD/HD NOMA in delay-limited transmission mode as below.

a) *FD NOMA case:* As suggested in Section III-A4, the system throughput of FD NOMA with direct link is given by

$$R_{i,dir}^{FD} = (1 - P_{D_1}^{FD}) R_1 + (1 - P_{D_2,dir}^{FD}) R_2, \quad (29)$$

where $P_{D_1}^{FD}$ and $P_{D_2,dir}^{FD}$ can be obtained from (10) and (27), respectively.

b) *HD NOMA case:* Similar to (29), the system throughput of HD NOMA with direct link is given by

$$R_{i,dir}^{HD} = (1 - P_{D_1}^{HD}) R_1 + (1 - P_{D_2,dir}^{HD}) R_2, \quad (30)$$

where $P_{D_1}^{HD}$ and $P_{D_2,dir}^{HD}$ can be obtained from (12) and [25, Eq. (11)].

IV. ERGODIC RATE

When user's rates are determined by their channel conditions, the ergodic sum rate is an important metric for performance evaluation. Hence the performance of FD/HD user relaying are characterized in terms of ergodic sum rates in the following.

A. *User Relaying without Direct Link*

1) *Ergodic Rate of D_1 :* On the condition that D_1 can detect x_2 , the achievable rate of D_1 can be written as $R_{D_1} = \log(1 + \gamma_{D_1})$. The ergodic rate of D_1 for FD NOMA can be obtained in the following theorem.

Theorem 4. *The closed-form expression of ergodic rate for D_1 without direct link for FD NOMA is given by*

$$R_{D_1}^{FD} = \frac{a_1 \Omega_1}{\ln 2 (\Omega_{LI} - a_1 \Omega_1)} \left[e^{\frac{1}{a_1 \rho \Omega_1}} \text{Ei} \left(\frac{-1}{a_1 \rho \Omega_1} \right) \right. \\ \left. - e^{\frac{1}{\rho \Omega_{LI}}} \text{Ei} \left(\frac{-1}{\rho \Omega_{LI}} \right) \right]. \quad (31)$$

Proof: See Appendix B. ■

As such, we can derive the ergodic rate of D_1 for HD NOMA in the following corollary.

Corollary 3. *The ergodic rate of D_1 for HD NOMA is given by*

$$R_{D_1}^{HD} = \frac{-e^{\frac{1}{a_1 \rho \Omega_1}} \text{Ei} \left(\frac{-1}{a_1 \rho \Omega_1} \right)}{2 \ln 2}. \quad (32)$$

2) *Ergodic Rate of D_2 :* Since x_2 should be detected at D_2 as well as at D_1 for SIC, the achievable rate of D_2 without direct link for FD NOMA is written as $R_{D_2} = \log(1 + \min(\gamma_{D_2 \rightarrow D_1}, \gamma_{2,D_2}))$. The corresponding ergodic rate is given by

$$R_{D_2,nodir}^{FD} = \frac{1}{\ln 2} \int_0^\infty \frac{1 - F_{X_1}(x_1)}{1 + x_1} dx_1, \quad (33)$$

where $X_1 = \min\left(\frac{|h_1|^2 a_2 \rho}{|h_1|^2 a_1 \rho + \varpi |h_{LI}|^2 \rho + 1}, |h_2|^2 \rho\right)$ with $\varpi = 1$. Obviously, it is difficult to obtain the CDF of X_1 . However, in order to derive an accurate closed-form expression for the ergodic rate applicable to high SNR region, the following theorem provides the high SNR approximation.

Theorem 5. *The asymptotic expression for ergodic rate of D_2 without direct link for FD NOMA in the high SNR region is given by*

$$R_{D_2,nodir}^{FD,\infty} = \frac{1}{\ln 2} \left\{ e^{\frac{1}{\rho \Omega_2}} \left[\text{Ei} \left(\frac{-1}{\rho a_1 \Omega_2} \right) - \text{Ei} \left(\frac{-1}{\rho \Omega_2} \right) \right] \right. \\ \times \left(\frac{\Omega_1}{a_2 \Omega_1 - \xi} \right) - \frac{e^{\frac{a_2 \Omega_1}{\rho \Omega_2 \xi}}}{\xi} \left[\text{Ei} \left(-\frac{a_2 \xi + a_1 a_2 \Omega_1}{\rho a_1 \xi \Omega_2} \right) \right. \\ \left. \left. - \text{Ei} \left(-\frac{a_2 \Omega_1}{\rho \Omega_2 \xi} \right) \right] \left(\frac{a_1 a_2 \Omega_1^2 + a_2 \Omega_1 \xi}{a_2 \Omega_1 - \xi} \right) \right\}, \quad (34)$$

where $\xi = (\Omega_{LI} - a_1\Omega_1)$.

Proof: See Appendix C. ■

For $\varpi = 0$, the ergodic rate of D_2 without direct link for HD NOMA is given by

$$R_{D_2, nodir}^{HD} = \frac{1}{2 \ln 2} \int_0^{\frac{a_2}{a_1}} \frac{e^{-\frac{y}{\rho(a_2 - y a_1)\Omega_1} - \frac{y}{\rho\Omega_2}}}{1 + y} dy. \quad (35)$$

As can be seen from the above expression, (35) does not have a closed-form solution. Corollary 4 gives the high SNR approximation.

Corollary 4. *The asymptotic expression for ergodic rate of D_2 without direct link for HD NOMA in the high SNR region is given by*

$$R_{D_2, nodir}^{HD, \infty} = \frac{e^{\frac{1}{\rho\Omega_2}}}{2 \ln 2} \left[\text{Ei} \left(\frac{-1}{\rho a_1 \Omega_2} \right) - \text{Ei} \left(\frac{-1}{\rho \Omega_2} \right) \right]. \quad (36)$$

Proof: See Appendix D. ■

3) *Slope Analysis:* In this subsection, the high SNR slope is evaluated, which is the key parameter determining ergodic rate in high SNR region. The high SNR slope is defined as

$$S = \lim_{\rho \rightarrow \infty} \frac{R_D^\infty(\rho)}{\log(\rho)}. \quad (37)$$

a) D_1 for FD NOMA case: Based on (31), when $\rho \rightarrow \infty$, by using $\text{Ei}(-x) \approx \ln(x) + C$ [38, Eq. (8.212.1)] and $e^{-x} \approx 1 - x$, where C is the Euler constant, the asymptotic ergodic rate of D_1 for FD NOMA is given by

$$R_{D_1}^{FD, \infty} = \frac{a_1 \Omega_1}{\ln 2 (\Omega_{LI} - a_1 \Omega_1)} \left[\left(1 + \frac{1}{a_1 \rho \Omega_1} \right) \left(\ln \left(\frac{1}{a_1 \rho \Omega_1} \right) + C \right) - \left(1 + \frac{1}{\rho \Omega_{LI}} \right) \left(\ln \left(\frac{1}{\rho \Omega_{LI}} \right) + C \right) \right]. \quad (38)$$

Substituting (38) into (37), we can obtain $S_{D_1}^{FD} = 0$.

b) D_1 for HD NOMA case: Based on (32), the asymptotic ergodic rate of D_1 for HD NOMA in the high SNR region is given by

$$R_{D_1}^{HD, \infty} = \frac{-1}{2 \ln 2} \left(1 - \frac{1}{a_1 \rho \Omega_1} \right) \left[\ln \left(\frac{1}{a_1 \rho \Omega_1} \right) + C \right]. \quad (39)$$

Substituting (39) into (37), we can obtain $S_{D_1}^{HD} = \frac{1}{2}$.

c) D_2 for FD NOMA case: Based on above analysis, substituting (34) into (37), we can obtain $S_{D_2, nodir}^{FD} = 0$.

d) D_2 for HD NOMA case: Such as (IV-A3c), substituting (36) into (37), we can obtain $S_{D_2, nodir}^{HD} = 0$.

Remark 5. *Based on above analysis, the ergodic rate of D_2 converges to a throughput ceiling in the high SNR region for FD/HD NOMA without direct link.*

Combing (34) and (38), the asymptotic expression for ergodic sum rate of FD NOMA without direct link is expressed

as

$$R_{sum, nodir}^{FD, \infty} = \frac{a_1 \Omega_1}{\ln 2 (\Omega_{LI} - a_1 \Omega_1)} \left[\left(1 + \frac{1}{a_1 \rho \Omega_1} \right) \times \left(\ln \left(\frac{1}{a_1 \rho \Omega_1} \right) + C \right) - \left(1 + \frac{1}{\rho \Omega_{LI}} \right) \left(\ln \left(\frac{1}{\rho \Omega_{LI}} \right) + C \right) \right] + \frac{1}{\ln 2} \left\{ e^{\frac{1}{\rho\Omega_2}} \left[\text{Ei} \left(\frac{-1}{\rho a_1 \Omega_2} \right) - \text{Ei} \left(\frac{-1}{\rho \Omega_2} \right) \right] \left(\frac{\Omega_1}{a_2 \Omega_1 - \xi} \right) + \frac{e^{\frac{a_2 \Omega_1}{\rho \Omega_2 \xi}}}{\xi} \left[\text{Ei} \left(\frac{-a_2 \Omega_1}{\rho \Omega_2 \xi} \right) - \text{Ei} \left(\frac{-a_2 \xi - a_1 a_2 \Omega_1}{\rho a_1 \xi \Omega_2} \right) \right] \times \left(\frac{a_1 a_2 \Omega_1^2 + a_2 \Omega_1 \xi}{a_2 \Omega_1 - \xi} \right) \right\}. \quad (40)$$

Similarly, combing (36) and (39), the asymptotic expression for ergodic sum rate of HD NOMA without direct link is expressed as

$$R_{sum, nodir}^{HD, \infty} = \frac{-1}{2 \ln 2} \left(1 - \frac{1}{a_1 \rho \Omega_1} \right) \left[\ln \left(\frac{1}{a_1 \rho \Omega_1} \right) + C \right] + \frac{e^{\frac{1}{\rho\Omega_2}}}{2 \ln 2} \left[\text{Ei} \left(\frac{-1}{\rho a_1 \Omega_2} \right) - \text{Ei} \left(\frac{-1}{\rho \Omega_2} \right) \right]. \quad (41)$$

4) *Throughput Analysis:* In this subsection, the throughput in delay-tolerant transmission for FD/HD NOMA are presented, respectively.

a) *FD NOMA case:* In this mode, the throughput is determined by evaluating the ergodic rate. Using (31) and (33), the system throughput of FD NOMA without direct link is given by

$$R_{t, nodir}^{FD} = R_{D_1}^{FD} + R_{D_2, nodir}^{FD}. \quad (42)$$

b) *HD NOMA case:* Similar to (42), using (32) and (35), the system throughput of HD NOMA without direct link is given by

$$R_{t, nodir}^{HD} = R_{D_1}^{HD} + R_{D_2, nodir}^{HD}. \quad (43)$$

B. User Relaying with Direct Link

In this subsection, we investigate the ergodic rate of D_2 for FD/HD NOMA with direct link.

1) *Ergodic Rate of D_2 :* Assume that the signal x_2 from relaying and direct link can be detected at D_2 as well as at D_1 for SIC. Moreover, considering the effect of RI between these two links, the achievable rate of D_2 is written as $R_{D_2, dir}^{RI} = \log \left(1 + \min \left(\gamma_{D_2 \rightarrow D_1}, \gamma_{D_1, D_2}^{RI} + \gamma_{D_2}^{RI} \right) \right)$. For the sake of simplicity, the achievable rate for D_2 can be further written as $R_{D_2, dir} = \log \left(1 + \min \left(\gamma_{D_2 \rightarrow D_1}, \gamma_{D_2}^{MRC} \right) \right)$. Hence, the ergodic rate of D_2 for FD NOMA is given by

$$R_{D_2, dir}^{FD} = \frac{1}{\ln 2} \int_0^\infty \frac{1 - F_{X_2}(x_2)}{1 + x_2} dx_2, \quad (44)$$

where $X_2 = \min \left(\frac{|h_1|^2 a_2 \rho}{|h_1|^2 a_1 \rho + \varpi |h_{LI}|^2 \rho + 1}, |h_2|^2 \rho + \frac{|h_0|^2 a_2 \rho}{|h_0|^2 a_1 \rho + 1} \right)$ with $\varpi = 1$. It is also difficult to obtain the CDF of X_2 and (44) has not closed-form expression. The following theorem provides the high SNR approximation.

Theorem 6. *The asymptotic expression for ergodic rate of D_2 with direct link for FD NOMA in the high SNR region is given by*

$$R_{D_2,dir}^{FD,\infty} = \frac{1}{\ln 2} \left\{ \ln \left(1 + \frac{a_2}{a_1} \right) \left(\frac{\Omega_1}{a_2\Omega_1 - \xi} \right) - \frac{1}{\xi} \ln \left(1 + \frac{\xi}{a_1\Omega_1} \right) \left(\frac{a_2\Omega_1\xi + a_1a_2\Omega_1^2}{a_2\Omega_1 - \xi} \right) \right\}. \quad (45)$$

Proof: See Appendix E. ■

For $\varpi = 0$, the ergodic rate of D_2 for HD NOMA with direct link is given by

$$R_{D_2,dir}^{HD} = \int_0^{\frac{a_2}{a_1}} \frac{e^{-\frac{y(\Omega_0 + \Omega_1)}{\rho(a_2 - a_1y)\Omega_0\Omega_1}}}{1 + y} dy + \int_0^{\frac{a_2}{a_1}} \int_0^{\frac{y}{\rho(a_2 - a_1y)}} \frac{e^{-\frac{x}{\Omega_0} - \frac{\gamma_{th_2}(xa_1\rho + 1) - xa_2\rho}{\rho(xa_1\rho + 1)\Omega_2} - \frac{y}{\rho(a_2 - a_1y)\Omega_1}}}{(1 + y)\Omega_0} dx dy. \quad (46)$$

To obtain the closed-form expression of ergodic rate for D_2 , the complicated integrals are required to be computed. Corollary 5 gives an efficient high SNR approximation.

Corollary 5. *The asymptotic expression for ergodic rate of D_2 with direct link for HD NOMA in the high SNR region is given by*

$$R_{D_2,dir}^{HD,\infty} = \frac{1}{2} \log \left(1 + \frac{a_2}{a_1} \right). \quad (47)$$

Combing (38) and (45), the asymptotic expression for the ergodic sum rate of FD NOMA with direct link is expressed as

$$R_{sum,dir}^{FD,\infty} = \frac{a_1\Omega_1}{\ln 2 (\Omega_{LI} - a_1\Omega_1)} \left[\left(1 + \frac{1}{a_1\rho\Omega_1} \right) \left(\ln \left(\frac{1}{a_1\rho\Omega_1} \right) + C \right) - \left(1 + \frac{1}{\rho\Omega_{LI}} \right) \left(\ln \left(\frac{1}{\rho\Omega_{LI}} \right) + C \right) \right] + \frac{1}{\ln 2} \times \left[\ln \left(1 + \frac{a_2}{a_1} \right) \left(\frac{\Omega_1}{a_2\Omega_1 - \xi} \right) - \frac{1}{\xi} \ln \left(1 + \frac{\xi}{a_1\Omega_1} \right) \right] \times \left(\frac{a_2\Omega_1\xi + a_1a_2\Omega_1^2}{a_2\Omega_1 - \xi} \right) \quad (48)$$

In the same way, combining (39) and (47), the asymptotic expression for ergodic sum rate of HD NOMA with direct link is expressed as

$$R_{sum,dir}^{HD,\infty} = \frac{-1}{2\ln 2} \left(1 - \frac{1}{a_1\rho\Omega_1} \right) \left[\ln \left(\frac{1}{a_1\rho\Omega_1} \right) + C \right] + \frac{1}{2} \log \left(1 + \frac{a_2}{a_1} \right). \quad (49)$$

2) *Slope Analysis:* Based on the derived asymptotic ergodic rates, the high SNR slopes of D_2 with direct link are characterized in the following.

a) *D_2 for FD NOMA case:* Substituting (45) into (37), we can obtain $S_{D_2,dir}^{FD} = 0$.

b) *D_2 for HD NOMA case:* Such as (IV-B2a), substituting (47) into (37), we can obtain $S_{D_2,dir}^{HD} = 0$.

Remark 6. *Based on above derived results, the ergodic rate of D_2 also converge to a throughput ceiling in the high SNR region with direct link for FD/HD NOMA. The user of direct link is incapable of assisting D_2 to obtain the additional high SNR slope.*

3) *Throughput Analysis:*

a) *FD NOMA case:* As suggested in Section IV-A4, in delay-tolerant transmission mode, using (31) and (44), the system throughput for FD NOMA with direct link is given by

$$R_{t,dir}^{FD} = R_{D_1}^{FD} + R_{D_2,dir}^{FD}. \quad (50)$$

b) *HD NOMA case:* Similar to (50), using (32) and (46), the system throughput for HD NOMA with direct link is given by

$$R_{t,dir}^{HD} = R_{D_1}^{HD} + R_{D_2,dir}^{HD}. \quad (51)$$

As shown in TABLE I, the diversity orders and high SNR slopes of two users for FD/HD NOMA are summarized to illustrate the comparison between them. In TABLE I, we use ‘‘D’’ and ‘‘S’’ to represent the diversity order and high SNR slope, respectively.

Duplex mode	Link mode	User	D	S
FD NOMA	Nodirect	User1	0	0
		User2	0	0
	Direct	User1	0	0
		User2	1	0
HD NOMA	Nodirect	User1	1	$\frac{1}{2}$
		User2	1	0
	Direct	User1	1	$\frac{1}{2}$
		User2	2	0

TABLE I: Diversity order and high SNR slope for FD/HD NOMA systems.

V. ENERGY EFFICIENCY

Based on throughput analysis, we aim to provide the system energy efficiency (EE) considering user relaying for FD/HD NOMA systems.

The definition of energy efficiency is given by

$$\eta_{EE} = \frac{\text{Total data rate}}{\text{Total energy consumption}}. \quad (52)$$

For FD/HD NOMA energy efficiency, the total data rate is denoted as sum throughput from the BS to D_1 and D_2 and from D_1 to D_2 . The total power consumption is denoted as the sum of the transmitted power P_s at the BS and P_r at D_1 . Based on results in Section III-A4, III-B3 and IV-A4, IV-B3, the energy efficiency of user relaying for FD/HD NOMA systems are expressed as

$$\eta_{\Phi}^{FD} = \frac{R_{\Phi}^{FD}}{TP_s + TP_r}, \quad (53)$$

and

$$\eta_{\Phi}^{HD} = \frac{2R_{\Phi}^{HD}}{TP_s + TP_r}, \quad (54)$$

respectively. T denotes the transmission time for the entire communication process. $\Phi \in (l_{nodir}, l_{dir}, t_{nodir}, t_{dir})$. $\eta_{l_{nodir}}$ and $\eta_{l_{dir}}$ are system energy efficiencies without/with direct link in delay-limited transmission mode, respectively. $\eta_{t_{nodir}}$ and $\eta_{t_{dir}}$ are system energy efficiencies without/with direct link in delay-tolerant transmission mode, respectively.

VI. NUMERICAL RESULTS

In this section, simulation results are provided to validate our analytical expressions derived in the previous section, and further evaluate the performance of FD/HD user relaying in NOMA systems. Without loss of generality, we assume that the distance between BS and D_2 is normalized to unity, i.e. $\Omega_0 = 1$. $\Omega_1 = d^{-\alpha}$ and $\Omega_2 = (1-d)^{-\alpha}$, where d is the normalised distance between BS and D_1 setting to be $d = 0.3$ and α is the pathloss exponent setting to be $\alpha = 2$. The power allocation coefficients of NOMA are $a_1 = 0.2$ and $a_2 = 0.8$ for D_1 and D_2 , respectively.

A. Without Direct Link

For user relaying without direct link, the target rate is set to be $R_1 = 3$, $R_2 = 0.5$ bit per channel use (BPCU) for D_1 and D_2 , respectively. The performance of conventional OMA is shown as a benchmark for comparison, in which the total communication process is finished in three slots. In the first slot, the BS sends information x_1 to D_1 and sends x_2 to D_1 in the second slot. In the last slot, D_1 decodes and forwards the information x_2 to D_2 .

1) *Outage Probability*: Fig. 2 plots the outage probability of two users versus SNR without direct link and the value of LI is assumed to be $\mathbb{E}\{|h_{LI}|^2\} = -15$ dB. The exact theoretical curves for the outage probability of two users for FD/HD NOMA are plotted according to (10), (14) and (12), (17), respectively. Obviously, the exact outage probability curves match precisely with the Monte Carlo simulation results. It is observed that the outage performance of FD NOMA exceeds HD NOMA and OMA on the condition of low SNR region. This is because LI is not dominant impact factor in the low SNR region for FD NOMA and answers the first question we raised in the introduction part. Especially, one can also observe that the outage behavior of D_2 for HD NOMA outperforms HD OMA [32, Eq. (8)]. The asymptotic outage probability curves of two users for HD NOMA are plotted according to (20) and (22), respectively. The asymptotic curves well approximate the exact performance curves in the high SNR region. It is shown that error floors exist in FD NOMA, which verify the conclusion in **Remark 3** and obtain zero diversity order. This is due to the fact that there is loop interference in FD NOMA. Another observation is that HD NOMA and OMA are superior to FD NOMA in the high SNR region. Therefore, we can select different operation mode for user relaying according to the different SNR levels in practical cooperative NOMA systems.

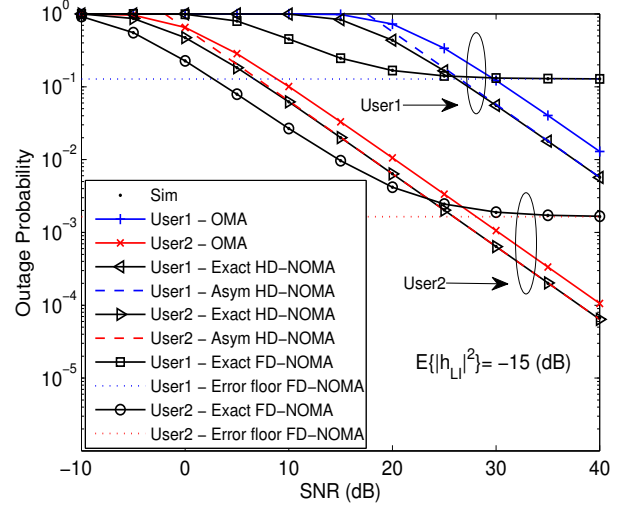


Fig. 2: Outage probability versus the transmit SNR without direct link.

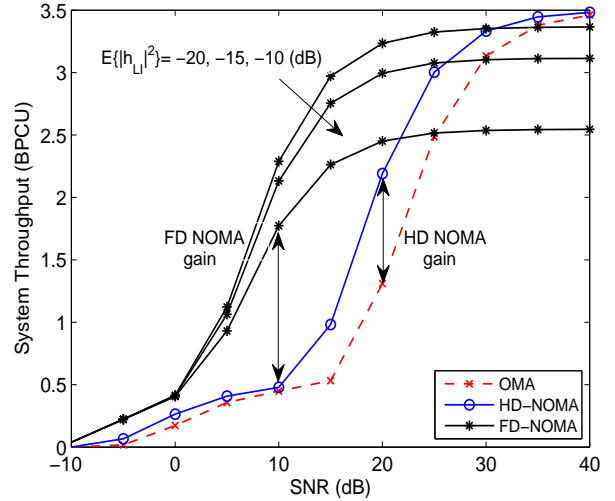


Fig. 3: System throughput in delay-limited transmission mode versus SNR with different values of LI without direct link.

Fig. 3 plots the system throughput versus SNR in delay-limited transmission mode without direct link. The solid curves represent throughput for FD/HD NOMA without direct link which are obtained from (23) and (24), respectively. We can observe that FD NOMA achieves a higher throughput than HD NOMA and OMA, since FD NOMA has the low values of LI. It is worth noting that increasing the values of LI from -20 dB to -10 dB reduce the system throughput in high SNR region. This is because FD NOMA converges to an error floor in high SNR region.

2) *Ergodic Rate*: Fig. 4 plots the ergodic sum rate of FD/HD NOMA without direct link versus SNR and the value of LI is assumed to be $\mathbb{E}\{|h_{LI}|^2\} = -10$ dB. The blue and red solid curves denote the achievable rates of D_1 for FD/HD NOMA, respectively. The dashdotted curves denote

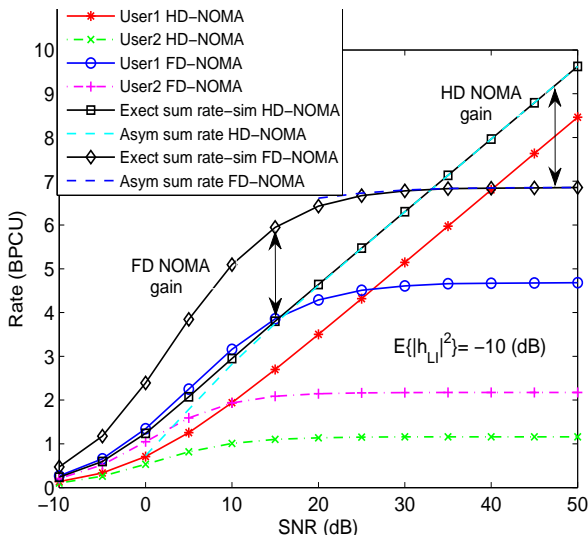


Fig. 4: Rates versus the transmit SNR without direct link.

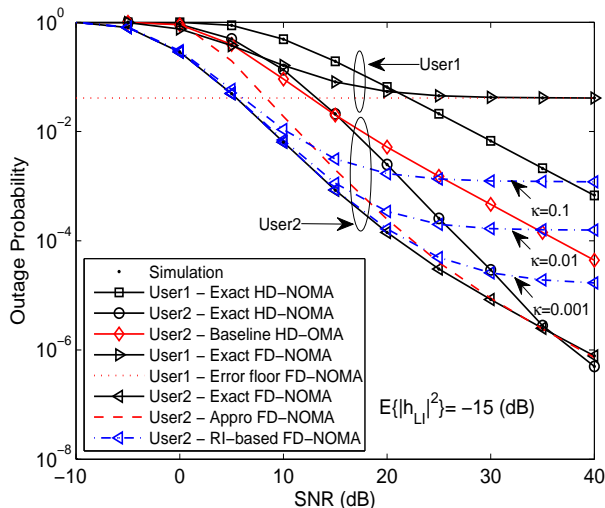


Fig. 5: Outage probability versus the transmit SNR with direct link.

the achievable rates of D_2 for FD/HD NOMA, respectively. One can observe that the achievable rate of D_1 for FD NOMA is superior to HD NOMA in the low SNR region. This phenomenon can be also explained is that LI has little effect on achievable rate of D_1 in the low SNR region. On the contrary, due to the influence of LI, the ergodic rate of D_1 converge to a throughput ceiling in the high SNR region. Another observation is that the achievable rate of D_2 for FD NOMA exceeds the HD NOMA. This is due to the fact that the communication process is completed over one slot time for FD NOMA. It is also shown that throughput ceilings exist in FD/HD NOMA for D_2 , which verify the conclusion in **Remark 5**. The dashed curves denote the asymptotic ergodic sum rate for FD/HD NOMA, corresponding to the analytical results derived in (40) and (41), respectively. An important observation is that FD NOMA can achieve the maximal

ergodic sum rate corresponding to HD NOMA and OMA in the low SNR region. The reason is that FD NOMA can improve system spectrum efficiency in the low SNR region. This phenomenon answers the third question we raised in the introduction part.

B. With Direct Link

For user relaying with direct link, the target rate is set to be $R_1 = 2$, $R_2 = 1$ BPCU for D_1 and D_2 , respectively. The performance of conventional HD NOMA is shown as a benchmark for comparison, which has been discussed in [25].

1) *Outage Probability*: Fig. 5 plots the outage probability of two users versus SNR and the value of LI is assumed to be $E\{|h_{LI}|^2\} = -15$ dB. The exact outage probability curves of two users for FD NOMA are given by Monte Carlo simulations and perfectly match with the analytical results derived in (10) and (27). The approximated outage probability curve for D_2 is plotted according to (28) is practically indistinguishable from the exact expression. We observe that D_2 obtains one diversity order by using the direct link, which overcomes the problem of zero diversity order inherent to FD cooperative systems. This phenomenon answers the second question we raised in the introduction part. More importantly, one can observe that the performance of FD NOMA is superior to HD NOMA in the low SNR region, whilst the performance is inferior to HD NOMA in the high SNR region. Additionally, for D_2 , considering the impact of RI between relaying link and direct link, we plots the corresponding outage probability of D_2 based on (25) denoted by blue dash-dotted curves. As can be seen from Fig. 5, these simulation results almost match with analytical result derived in (27) by utilizing the upper bound SINR in low SNR region. However, with the increase of RI levels κ , the RI-based simulation results for D_2 converge to a constant and provide an error floor in high SNR region. Hence, the effect of RI should be carefully addressed in practical FD NOMA systems. Another observation is that the outage behavior of D_2 for FD/HD NOMA outperforms HD OMA [39, Eq. (13)]. That is due to the fact that NOMA can provide more spectral efficiency compared to OMA.

Fig. 6 plots the outage probability of the two users versus different values of LI from -20 dB to -10 dB. We see that LI strongly affect the performance of FD NOMA systems. With the values of LI increasing, the superiority of FD NOMA is no longer apparent. Therefore, it is important to consider the influence of LI when designing practical FD NOMA systems. Fig. 7 plots system throughput versus SNR in delay-limited transmission mode with direct link. The solid curves, representing FD NOMA, is obtained from (29). The dashed curve, representing HD NOMA, is obtained from (30). Observe that FD NOMA also outperform HD NOMA in the low SNR region. The reason is that in low SNR region, the outage probability is small and has no effect on the throughput, which only depends on the fixed transmission rates at the BS.

2) *Ergodic Rate*: Fig. 8 plots the ergodic sum rate of HD/FD NOMA with direct link versus SNR and the value of LI is assumed to be $E\{|h_{LI}|^2\} = -10$ dB. The dashed

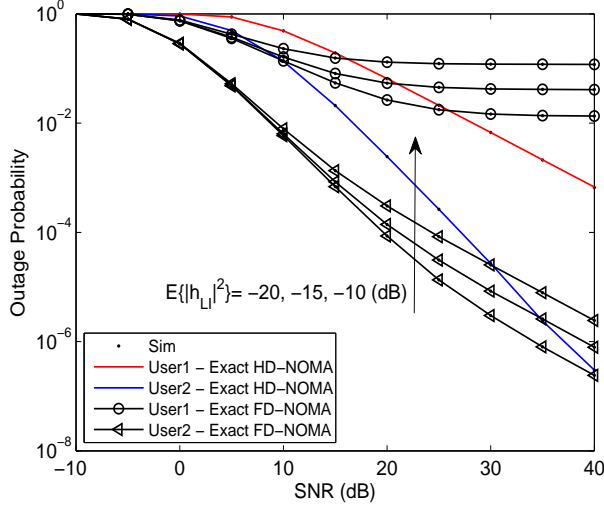


Fig. 6: Outage probability versus the transmit SNR for different values of LI with direct link.

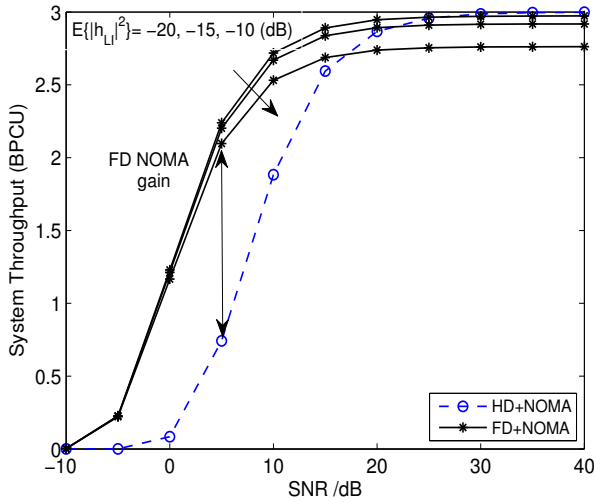


Fig. 7: System throughput in delay-limited transmission mode versus SNR with different LI with direct link.

curves denote the asymptotic ergodic sum rate for FD/HD NOMA based on the analytical results derived in (48) and (49), respectively. It is observed that the asymptotic ergodic sum rate is larger for FD/HD NOMA in the low SNR region. This can be explained as the direct link between BS and D_2 exists and improves system reliability. One can observed from figure, as the RI value increases, the achievable rate of D_2 becomes smaller, such as, setting κ from 0.5 to 1. In addition to consider the effect of LI, it is also important to design effective rake receiver at D_2 for FD NOMA system.

C. Energy Efficiency

Fig. 9 plots the system energy efficiency versus SNR in delay-limited transmission mode for user relaying in NOMA systems. The dashed curves, representing user relaying without

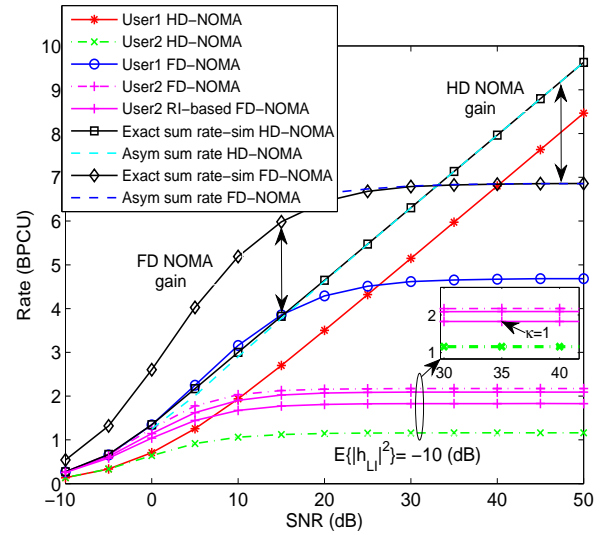


Fig. 8: Rates versus the transmit SNR with direct link.

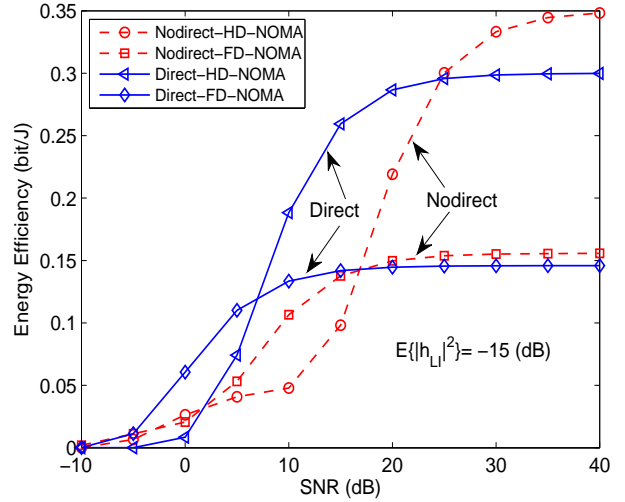


Fig. 9: System energy efficiency in delay-limited transmission mode, where $P_s = P_r = 10$ W, and $T = 1$.

direct link for FD/HD NOMA are obtained from (53), (23) and (54), (24) with throughput in delay-limited transmission mode, respectively. The solid curves, representing user relaying with direct link for FD/HD NOMA are obtained from (53), (29) and (54), (30) with throughput in transmission mode, respectively. It can be seen that the energy efficiency of user relaying for FD/HD NOMA in delay-limited transmission mode is $FD > HD$ in the low SNR region. The reason is that FD NOMA can achieve larger throughput than that of HD NOMA at this transmission mode. This phenomenon answers the fourth question we raised in the introduction part.

Fig. 10 plots the system energy efficiency versus SNR in delay-tolerant transmission mode for user relaying in NOMA systems. The dashed curves, representing user relaying without direct link for FD/HD NOMA are obtained from (40), (53) and (41), (54) with throughput in delay-tolerant mode, respectively.

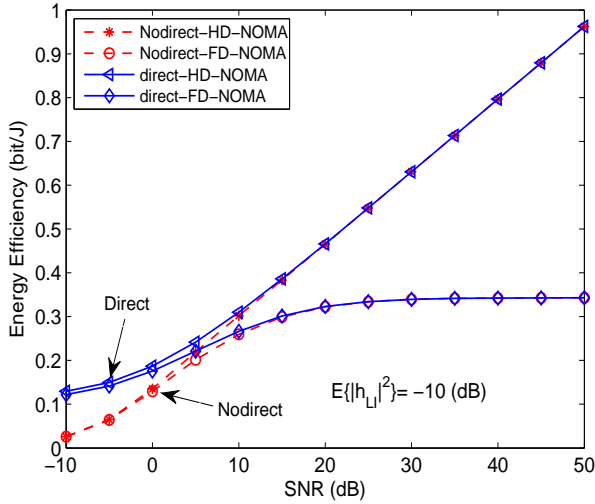


Fig. 10: System energy efficiency in delay-tolerant transmission mode, where $P_s = P_r = 10$ W, and $T = 1$.

The solid curves, representing user relaying with direct link for FD/HD NOMA are obtained from (48), (53) and (49), (54) with throughput in delay-tolerant mode, respectively. We observe that user relaying with direct link has a higher energy efficiency compared to without direct link for FD/HD NOMA in the low SNR region. This is because that the direct link improves system throughput at this transmission mode. Additionally, it is worth noting that HD NOMA achieves the higher system energy efficiency in the high SNR region. This is due to the fact that HD NOMA can provide a larger system throughput, while FD NOMA converges to the throughput ceiling in the high SNR region.

VII. CONCLUSION

This paper has investigated FD/HD user relaying in cooperative NOMA system and two cooperative relaying scenarios have been considered insightfully. The performance of FD/HD user relaying for NOMA system was characterized. The closed-form expressions of outage probability for two users have been derived. Due to the influence of LI, the diversity orders achieved by two user were zeros for FD NOMA. Therefore, the direct link between BS and far user was utilized to convey information and one diversity order was obtained for the far user. Based on the analytical results, it was shown that FD NOMA was superior to HD NOMA in low SNR region rather than in the high SNR region. The superior of FD NOMA was not apparent with the values of LI increasing. Furthermore, the expressions of ergodic sum rate for FD/HD user relaying were derived. The results showed that FD NOMA achieved a higher sum rate than HD NOMA in the low SNR region. In addition, the system energy efficiencies for FD/HD user relaying were discussed in different transmission modes.

APPENDIX A: PROOF OF THEOREM 3

Based on (26), the outage probability of D_2 can be expressed as

$$P_{D_2,dir}^{FD} = \underbrace{P_r(\gamma_{D_2}^{MRC} < \gamma_{th_2}^{FD})}_{J_{11}} \underbrace{P_r(\gamma_{D_2 \rightarrow D_1} > \gamma_{th_2}^{FD})}_{J_{12}} + \underbrace{P_r(\gamma_{1,D_2} < \gamma_{th_2}^{FD}, \gamma_{D_2 \rightarrow D_1} < \gamma_{th_2}^{FD})}_{J_{13}}. \quad (A.1)$$

Furthermore, substituting (2), (6) and (8) to (A.1), J_{11} and J_{12} can be calculated as

$$\begin{aligned} J_{11} &= P_r \left(|h_2|^2 < \frac{\gamma_{th_2}^{FD}}{\rho} - \frac{|h_0|^2 a_2}{|h_0|^2 a_1 \rho + 1}, |h_0|^2 < \tau_1 \right) \\ &= \int_0^{\tau_1} F_{|h_2|^2} \left(\frac{\gamma_{th_2}^{FD}}{\rho} - \frac{y a_2}{y a_1 \rho + 1} \right) f_{|h_0|^2}(y) dy \\ &= 1 - e^{-\frac{\tau_1}{\Omega_0}} - \underbrace{\int_0^{\tau_1} \frac{1}{\Omega_0} e^{-\frac{y}{\Omega_0}} e^{-\frac{1}{\Omega_2} \left(\frac{\gamma_{th_2}^{FD}}{\rho} - \frac{y a_2}{y a_1 \rho + 1} \right)} dy}_{\Theta_1}. \end{aligned} \quad (A.2)$$

Based on (A.2), using $x = y \rho a_1 + 1$, Θ_1 can be calculated as

$$\begin{aligned} \Theta_1 &= \frac{1}{\Omega_0} e^{-\frac{\gamma_{th_2}^{FD}}{\rho \Omega_2}} \int_1^{\tau_1 \rho a_1 + 1} e^{-\frac{x-1}{\rho a_1 \Omega_0}} e^{-\frac{a_2(x-1)}{a_1 \rho \Omega_2 x}} dx \\ &= \frac{e^\varphi}{\phi_2} \sum_{n=0}^{\infty} \frac{(-1)^n}{n! (\Omega_0 \rho a_1)^n} \underbrace{\int_1^{\tau_1 \rho a_1 + 1} x^n e^{-\frac{x}{a_1 \rho \Omega_2 x}} dx}_{\Theta_2}, \end{aligned} \quad (A.3)$$

where $\varphi = \frac{1}{\rho a_1 \Omega_0} - \frac{\gamma_{th_2}^{FD}}{\rho \Omega_2} - \phi_1$, $\phi_1 = \frac{-a_2}{a_1 \rho \Omega_2}$ and $\phi_2 = a_1 \rho \Omega_0$. Note that (A.3) is obtained by using Binomial theorem.

Furthermore, using $z = \frac{1}{x}$, Θ_2 is given by

$$\begin{aligned} \Theta_2 &= \int_{\frac{1}{\tau_1 \rho a_1 + 1}}^1 \frac{1}{z^{n+2}} e^{-\frac{a_2 z}{a_1 \rho \Omega_2}} dz \\ &= \frac{(-1)^{2n+1} \phi_1^{n+1}}{(n+1)!} (\text{Ei}(\psi) - \text{Ei}(\phi_1)) \\ &\quad + \sum_{k=0}^n \frac{(1 + a_1 \rho \tau_1)^{n+1} e^\psi \psi^k - e^{\phi_1} \phi_1^k}{(n+1) n \cdots (n+1-k)}, \end{aligned} \quad (A.4)$$

where (A.4) can be obtained by using [38, Eq. (3.351.4)].

Substituting (A.3) into (A.2), J_{11} is written as

$$J_{11} = \left\{ 1 - e^{-\frac{\tau_1}{\Omega_0}} - \sum_{n=0}^{\infty} \frac{(-1)^n e^\varphi}{n! \phi_2^{n+1}} \left[\frac{(-1)^{2n+1} \phi_1^{n+1}}{(n+1)!} (\text{Ei}(\psi) - \text{Ei}(\phi_1)) + \sum_{k=0}^n \frac{(1 + a_1 \rho \tau_1)^{n+1} e^\psi \psi^k - e^{\phi_1} \phi_1^k}{(n+1) n \cdots (n+1-k)} \right] \right\}. \quad (A.5)$$

After some algebraic manipulations, J_{12} is calculated as

$$J_{12} = \int_0^\infty \frac{1}{\Omega_{LI}} e^{-\frac{y}{\Omega_{LI}}} \int_{\tau_1(y\rho+1)}^\infty \frac{1}{\Omega_1} e^{-\frac{x}{\Omega_1}} dx dy = \chi e^{-\frac{\tau_1}{\Omega_1}}, \quad (A.6)$$

where $\chi = \frac{\Omega_1}{\Omega_1 + \tau_1 \rho \Omega_{LI}}$.

Similarly, J_{13} is given by

$$J_{13} = \left(1 - e^{-\frac{\tau_1}{\Omega_1}}\right) \left(1 - \chi e^{-\frac{\tau_1}{\Omega_1}}\right). \quad (\text{A.7})$$

Combining (A.5), (A.6) and (A.7), we can obtain (27).
The proof is completed.

APPENDIX B: PROOF OF THEOREM 4

To obtain (31), the ergodic rate of D_1 for FD NOMA is expressed as

$$\begin{aligned} R_{D_1}^{FD} &= \mathbb{E} \left[\log \left(1 + \frac{|h_1|^2 a_1 \rho}{\underbrace{\varpi |h_{LI}|^2 \rho + 1}_X} \right) \right] \\ &= \frac{1}{\ln 2} \int_0^\infty \frac{1 - F_X(x)}{1+x} dx \end{aligned} \quad (\text{B.1})$$

where $\varpi = 1$.

The CDF of X is calculated as follows

$$\begin{aligned} F_X(x) &= \Pr \left(|h_1|^2 < \frac{x \left(|h_{LI}|^2 \rho + 1 \right)}{a_1 \rho} \right) \\ &= \int_0^\infty \frac{1}{\Omega_{LI}} e^{-\frac{z}{\Omega_{LI}}} \int_0^{\frac{x(z\rho+1)}{a_1\rho}} \frac{1}{\Omega_1} e^{-\frac{y}{\Omega_1}} dy dz \\ &= 1 - \frac{a_1 \Omega_1}{x \Omega_{LI} + a_1 \Omega_1} e^{-\frac{x}{a_1 \rho \Omega_1}}. \end{aligned} \quad (\text{B.2})$$

Substituting (B.2) into (B.1), the ergodic rate of D_1 is written as

$$\begin{aligned} R_{D_1}^{FD} &= \frac{1}{\ln 2} \int_0^\infty \frac{1}{1+x} \frac{a_1 \Omega_1}{a_1 \Omega_1 + x \Omega_{LI}} e^{-\frac{x}{a_1 \rho \Omega_1}} dx \\ &= \frac{1}{\ln 2} \int_0^\infty \underbrace{\frac{-a_1 \Omega_1 e^{-\frac{x}{a_1 \rho \Omega_1}}}{(1+x)(\Omega_{LI} - a_1 \Omega_1)}}_{J_1} dx \\ &\quad + \frac{1}{\ln 2} \int_0^\infty \underbrace{\frac{a_1 \Omega_1 \Omega_{LI} e^{-\frac{x}{a_1 \rho \Omega_1}}}{(a_1 \Omega_1 + x \Omega_{LI})(\Omega_{LI} - a_1 \Omega_1)}}_{J_2} dx. \end{aligned} \quad (\text{B.3})$$

Based on [38, Eq. (3.352.4)] and applying some polynomial expansion manipulations, J_1 and J_2 are given by

$$J_1 = \frac{a_1 \Omega_1 e^{\frac{1}{a_1 \rho \Omega_1}}}{\Omega_{LI} - a_1 \Omega_1} \text{Ei} \left(\frac{-1}{a_1 \rho \Omega_1} \right), \quad (\text{B.4})$$

and

$$J_2 = \frac{a_1 \Omega_1 e^{\frac{1}{\rho \Omega_{LI}}}}{\Omega_{LI} - a_1 \Omega_1} \text{Ei} \left(\frac{-1}{\rho \Omega_{LI}} \right). \quad (\text{B.5})$$

Substituting (B.4) and (B.5) into (B.3), we can obtain (31).
The proof is completed.

APPENDIX C: PROOF OF THEOREM 5

The proof starts by providing the ergodic rate of D_2 as follows:

$$R_{D_2, \text{nodir}}^{FD} = \mathbb{E} \left[\log \left(1 + \underbrace{\min(\gamma_{D_2 \rightarrow D_1}, \gamma_{2, D_2})}_{J_1} \right) \right], \quad (\text{C.1})$$

where $\varpi = 1$. We focus on the high SNR approximation of J_1 , which is given by

$$J_1 \approx \min \left(\underbrace{\frac{|h_1|^2 a_2}{|h_1|^2 a_1 + |h_{LI}|^2}, |h_2|^2 \rho}_Y \right). \quad (\text{C.2})$$

The CDF of Y is expressed as

$$F_Y(y) = 1 - \underbrace{\Pr(|h_2|^2 \rho > y)}_{\Theta_1} \underbrace{\Pr \left(\frac{|h_1|^2 a_2}{|h_1|^2 a_1 + |h_{LI}|^2} > y \right)}_{\Theta_2}. \quad (\text{C.3})$$

Θ_1 and Θ_2 are given by

$$\Theta_1 = 1 - e^{-\frac{y}{\rho \Omega_2}} \text{U}(y), \quad (\text{C.4})$$

and

$$\Theta_2 = \frac{(a_2 - y a_1) \Omega_1}{(a_2 - y a_1) \Omega_1 + y \Omega_{LI}} \text{U} \left(\frac{a_2}{a_1} - y \right), \quad (\text{C.5})$$

respectively, where $\text{U}(x)$ is unit step function as

$$\text{U}(x) = \begin{cases} 1, & x > 0 \\ 0, & x < 0 \end{cases}.$$

Substituting (C.4) and (C.5) into (C.3), the CDF of Y is given by

$$F_Y(y) = 1 - \frac{e^{-\frac{y}{\rho \Omega_2}} (a_2 - x a_1) \Omega_1}{(a_2 - x a_1) \Omega_1 + x \Omega_{LI}} \text{U}(y) \text{U} \left(\frac{a_2}{a_1} - y \right). \quad (\text{C.6})$$

Base on (C.6), a high SNR approximation of the ergodic rate for D_2 is written as

$$\begin{aligned} R_{D_2, \text{nodir}}^{FD, \infty} &= \frac{1}{\ln 2} \int_0^{\frac{a_2}{a_1}} \frac{1}{1+y} \frac{e^{-\frac{y}{\rho \Omega_2}} (a_2 - y a_1) \Omega_1}{(a_2 - y a_1) \Omega_1 + y \Omega_{LI}} dy \\ &= \frac{1}{\ln 2} \left(\underbrace{\int_0^{\frac{a_2}{a_1}} \frac{1}{1+y} \frac{a_2 \Omega_1 e^{-\frac{y}{\rho \Omega_2}}}{y \xi + a_2 \Omega_1} dy}_{J_2} \right. \\ &\quad \left. - \underbrace{\int_0^{\frac{a_2}{a_1}} \frac{1}{1+y} \frac{y a_1 \Omega_1 e^{-\frac{y}{\rho \Omega_2}}}{y \xi + a_2 \Omega_1} dy}_{J_3} \right), \end{aligned} \quad (\text{C.7})$$

where $\xi = (\Omega_{LI} - a_1 \Omega_1)$.

Applying [38, Eq. (3.352.1)] and some polynomial expansion manipulations, J_2 and J_3 can be calculated as

$$\begin{aligned} J_2 &= \frac{a_2\Omega_1}{a_2\Omega_1 - \xi} \left(\int_0^{\frac{a_2}{a_1}} \frac{e^{-\frac{y}{\rho\Omega_2}}}{1+y} dy - \int_0^{\frac{a_2}{a_1}} \frac{\xi e^{-\frac{y}{\rho\Omega_2}}}{\xi y + a_2\Omega_1} dy \right) \\ &= \frac{a_2\Omega_1}{a_2\Omega_1 - \xi} \left\{ e^{\frac{1}{\rho\Omega_2}} \left[\text{Ei} \left(\frac{-1}{\rho a_1 \Omega_2} \right) - \text{Ei} \left(\frac{-1}{\rho \Omega_2} \right) \right] \right. \\ &\quad \left. - e^{\frac{a_2\Omega_1}{\rho\Omega_2\xi}} \left[\text{Ei} \left(-\frac{a_2\xi + a_1 a_2 \Omega_1}{\rho a_1 \xi \Omega_2} \right) - \text{Ei} \left(-\frac{a_2\Omega_1}{\rho \Omega_2 \xi} \right) \right] \right\}. \end{aligned} \quad (\text{C.8})$$

$$\begin{aligned} J_3 &= \frac{a_1\Omega_1}{\xi - a_2\Omega_1} \left(\int_0^{\frac{a_2}{a_1}} \frac{e^{-\frac{y}{\rho\Omega_2}}}{1+y} dy - \int_0^{\frac{a_2}{a_1}} \frac{a_2\Omega_1 e^{-\frac{y}{\rho\Omega_2}}}{\xi y + a_2\Omega_1} dy \right) \\ &= \frac{a_1\Omega_1}{\xi - a_2\Omega_1} \left\{ e^{\frac{1}{\rho\Omega_2}} \left[\text{Ei} \left(\frac{-1}{\rho a_1 \Omega_2} \right) - \text{Ei} \left(\frac{-1}{\rho \Omega_2} \right) \right] \right. \\ &\quad \left. - \frac{a_2\Omega_1 e^{\frac{a_2\Omega_1}{\rho\Omega_2\xi}}}{\xi} \left[\text{Ei} \left(-\frac{a_2\xi + a_1 a_2 \Omega_1}{\rho a_1 \xi \Omega_2} \right) - \text{Ei} \left(-\frac{a_2\Omega_1}{\rho \Omega_2 \xi} \right) \right] \right\}. \end{aligned} \quad (\text{C.9})$$

Substituting (C.8) and (C.9) into (C.7), we can obtain (34). The proof is completed.

APPENDIX D: PROOF OF COROLLARY 4

We can rewrite (35) as follows:

$$R_{D_2, \text{nodir}}^{HD} = \frac{1}{2} \mathbb{E} \left[\log \left(1 + \underbrace{\min(\gamma_{D_2 \rightarrow D_1}, \gamma_{2, D_2})}_{J_1} \right) \right], \quad (\text{D.1})$$

where $\varpi = 0$.

At the high SNR region, J_1 is approximated as

$$J_1 \approx \underbrace{\min \left(\frac{a_2}{a_1}, |h_2|^2 \rho \right)}_Y. \quad (\text{D.2})$$

Therefore, $F_Y(y) = (1 - e^{-\frac{y}{\rho\Omega_2}}) \text{U} \left(\frac{a_2}{a_1} - y \right)$ can be easily obtained. As such, the approximated ergodic rate of D_2 for HD NOMA at high SNR is given in (36).

APPENDIX E: PROOF OF THEOREM 6

The proof starts by providing the ergodic rate of D_2 as follows:

$$R_{D_2, \text{dir}}^{FD} = \mathbb{E} \left[\log \left(1 + \underbrace{\min(\gamma_{D_2 \rightarrow D_1}, \gamma_{D_2}^{MRC})}_{J_1} \right) \right], \quad (\text{E.1})$$

where $\varpi = 1$. We focus on the high SNR approximation of J_1 , which is given by

$$J_1 \approx \underbrace{\min \left(\frac{|h_1|^2 a_2}{|h_1|^2 a_1 + |h_{LI}|^2}, |h_2|^2 \rho + \frac{a_2}{a_1} \right)}_Y. \quad (\text{E.2})$$

The cumulative distribution function (CDF) of Y is expressed as

$$\begin{aligned} F_Y(y) &= 1 - \text{Pr} \left(\underbrace{|h_2|^2 \rho + \frac{a_2}{a_1}}_{\Theta_1} \geq y \right) \\ &\quad \times \text{Pr} \left(\underbrace{\frac{|h_1|^2 a_2}{|h_1|^2 a_1 + |h_{LI}|^2}}_{\Theta_2} \geq y \right). \end{aligned} \quad (\text{E.3})$$

Θ_1 and Θ_2 are given by

$$\Theta_1 = 1 - \text{U} \left(y - \frac{a_2}{a_1} \right) e^{-\frac{1}{\rho\Omega_2} \left(y - \frac{a_2}{a_1} \right)}, \quad (\text{E.4})$$

and

$$\Theta_2 = \text{U} \left(\frac{a_2}{a_1} - y \right) \frac{(a_2 - y a_1) \Omega_1}{(a_2 - y a_1) \Omega_1 + y \Omega_{LI}}, \quad (\text{E.5})$$

respectively.

Substituting (E.4) and (E.5) into (E.3), the CDF of Y is given by

$$F_Y(y) = 1 - \text{U} \left(\frac{a_2}{a_1} - y \right) \frac{(a_2 - y a_1) \Omega_1}{(a_2 - y a_1) \Omega_1 + y \Omega_{LI}}. \quad (\text{E.6})$$

Base on (E.6), a high SNR approximation of the ergodic rate for D_2 is written as

$$\begin{aligned} R_{D_2, \text{dir}}^{FD, \infty} &= \frac{1}{\ln 2} \int_0^{\frac{a_2}{a_1}} \frac{1}{1+y} \frac{(a_2 - y a_1) \Omega_1}{(a_2 - y a_1) \Omega_1 + y \Omega_{LI}} dy \\ &= \frac{1}{\ln 2} \left(\underbrace{\int_0^{\frac{a_2}{a_1}} \frac{a_2 \Omega_1}{(1+y)(y\xi + a_2 \Omega_1)} dy}_{J_2} \right. \\ &\quad \left. - \underbrace{\int_0^{\frac{a_2}{a_1}} \frac{y a_1 \Omega_1}{(1+y)(y\xi + a_2 \Omega_1)} dy}_{J_3} \right), \end{aligned} \quad (\text{E.7})$$

where $\xi = (\Omega_{LI} - a_1 \Omega_1)$.

After some algebraic manipulations, J_2 and J_3 are obtained as follows:

$$J_2 = \frac{a_2 \Omega_1}{a_2 \Omega_1 - \xi} \left[\ln \left(1 + \frac{a_2}{a_1} \right) - \ln \left(1 + \frac{\xi}{a_1 \Omega_1} \right) \right]. \quad (\text{E.8})$$

$$J_3 = \frac{a_1 \Omega_1}{a_2 \Omega_1 - \xi} \left[\frac{a_2 \Omega_1}{\xi} \ln \left(1 + \frac{\xi}{a_1 \Omega_1} \right) - \ln \left(1 + \frac{a_2}{a_1} \right) \right]. \quad (\text{E.9})$$

Substituting (E.8) and (E.9) into (E.7), we can obtain (45). The proof is completed.

REFERENCES

- [1] X. Yue, Y. Liu, S. Kang, A. Nallanathan, and Z. Ding, "Outage performance of full/half-duplex user relaying in NOMA systems," in *IEEE Proc. of International Commun. Conf. (ICC)*, Paris, FRA, May, 2017, pp. 1–6.
- [2] Y. Cai, Z. Qin, F. Cui, G. Y. Li, and J. A. McCann, "Modulation and multiple access for 5G networks," *CoRR*, vol. abs/1702.07673, 2017. [Online]. Available: <https://arxiv.org/abs/1702.07673>

- [3] “Proposed solutions for new radio access, Mobile and wireless communications Enablers for the Twenty-twenty Information Society (METIS), Deliverable D.2.4, Feb. 2015.”
- [4] Y. Saito, Y. Kishiyama, A. Benjebbour, T. Nakamura, A. Li, and K. Higuchi, “Non-orthogonal multiple access (NOMA) for cellular future radio access,” in *Proc. IEEE Vehicular Technology Conference (VTC Spring)*, Dresden, GRE, Jun. 2013, pp. 1–5.
- [5] H. Nikopour and H. Baligh, “Sparse code multiple access,” in *Proc. IEEE Annual International Symposium on Personal, Indoor, and Mobile Radio Communications (PIMRC)*, London, UK, Sep. 2013, pp. 332–336.
- [6] S. Chen, B. Ren, Q. Gao, S. Kang, S. Sun, and K. Niu, “Pattern division multiple access PDMA - A novel nonorthogonal multiple access for fifth-generation radio networks,” *IEEE Trans. Veh. Technol.*, vol. 66, no. 4, pp. 3185–3196, Apr. 2017.
- [7] Z. Yuan, G. Yu, W. Li, Y. Yuan, X. Wang, and J. Xu, “Multi-user shared access for internet of things,” in *Proc. IEEE Vehicular Technology Conference (VTC Spring)*, Nanjing, CHN, May. 2016, pp. 1–5.
- [8] “3rd Generation Partnership Project (3GPP), “Study on downlink multiuser superposition transmission for LTE,” Mar. 2015.”
- [9] Z. Ding, Y. Liu, J. Choi, Q. Sun, M. Elkashlan, I. Chih-Lin, and H. V. Poor, “Application of non-orthogonal multiple access in LTE and 5G networks,” *IEEE Commun. Mag.*, vol. 55, no. 2, pp. 185–191, Feb. 2017.
- [10] M. Al-Imari, P. Xiao, M. A. Imran, and R. Tafazolli, “Uplink non-orthogonal multiple access for 5G wireless networks,” in *Proc. IEEE International Symposium on Wireless Communications Systems (ISWCS)*, Barcelona, ESP, Aug. 2014, pp. 781–785.
- [11] N. Zhang, J. Wang, G. Kang, and Y. Liu, “Uplink nonorthogonal multiple access in 5G systems,” *IEEE Commun. Lett.*, vol. 20, no. 3, pp. 458–461, Mar. 2016.
- [12] Z. Ding, Z. Yang, P. Fan, and H. V. Poor, “On the performance of non-orthogonal multiple access in 5G systems with randomly deployed users,” *IEEE Signal Process. Lett.*, vol. 21, no. 12, pp. 1501–1505, Dec. 2014.
- [13] Z. Ding, P. Fan, and H. V. Poor, “Impact of user pairing on 5G non-orthogonal multiple-access downlink transmissions,” *IEEE Trans. Veh. Technol.*, vol. 65, no. 8, pp. 6010–6023, Aug. 2016.
- [14] Y. Liu, Z. Ding, M. Elkashlan, and J. Yuan, “Non-orthogonal multiple access in large-scale underlay cognitive radio networks,” *IEEE Trans. Veh. Technol.*, vol. 65, no. 12, pp. 10 152–10 157, Dec. 2016.
- [15] Y. Tian, S. Lu, A. Nix, and M. Beach, “A novel opportunistic NOMA in downlink coordinated multi-point networks,” in *Proc. IEEE Vehicular Technology Conference (VTC Fall)*, Boston, USA, Sep. 2015, pp. 1–5.
- [16] Z. Yang, Z. Ding, P. Fan, and Z. Ma, “Outage performance for dynamic power allocation in hybrid non-orthogonal multiple access systems,” *IEEE Commun. Lett.*, vol. 20, no. 8, pp. 1695–1698, Aug. 2016.
- [17] P. Botsinis, D. Alanis, Z. Babar, H. Nguyen, D. Chandra, S. X. Ng, and L. Hanzo, “Quantum-aided multi-user transmission in non-orthogonal multiple access systems,” *IEEE Access*, to appear in 2016.
- [18] J. Choi, “On the power allocation for a practical multiuser superposition scheme in NOMA systems,” *IEEE Commun. Lett.*, vol. 20, no. 3, pp. 438–441, Mar. 2016.
- [19] Y. Liu, Z. Qin, M. Elkashlan, Y. Gao, and L. Hanzo, “Enhancing the physical layer security of non-orthogonal multiple access in large-scale networks,” *IEEE Trans. Wireless Commun.*, vol. 16, no. 3, pp. 1656–1672, Mar. 2017.
- [20] J. N. Laneman, D. N. C. Tse, and G. W. Wornell, “Cooperative diversity in wireless networks: Efficient protocols and outage behavior,” *IEEE Trans. Inf. Theory*, vol. 50, no. 12, pp. 3062–3080, Dec. 2004.
- [21] J. Choi, “Non-orthogonal multiple access in downlink coordinated two-point systems,” *IEEE Commun. Lett.*, vol. 18, no. 2, pp. 313–316, Feb. 2014.
- [22] J. B. Kim and I. H. Lee, “Non-orthogonal multiple access in coordinated direct and relay transmission,” *IEEE Commun. Lett.*, vol. 19, no. 11, pp. 2037–2040, Nov. 2015.
- [23] —, “Capacity analysis of cooperative relaying systems using non-orthogonal multiple access,” *IEEE Commun. Lett.*, vol. 19, no. 11, pp. 1949–1952, Nov. 2015.
- [24] J. Men, J. Ge, and C. Zhang, “Performance analysis of nonorthogonal multiple access for relaying networks over nakagami- m fading channels,” *IEEE Trans. Veh. Technol.*, vol. 66, no. 2, pp. 1200–1208, Feb. 2017.
- [25] Z. Ding, M. Peng, and H. V. Poor, “Cooperative non-orthogonal multiple access in 5G systems,” *IEEE Commun. Lett.*, vol. 19, no. 8, pp. 1462–1465, Aug. 2015.
- [26] Y. Liu, Z. Ding, M. Elkashlan, and H. V. Poor, “Cooperative non-orthogonal multiple access with simultaneous wireless information and power transfer,” *IEEE J. Sel. Areas Commun.*, vol. 34, no. 4, pp. 938–953, Apr. 2016.
- [27] H. Ju, E. Oh, and D. Hong, “Improving efficiency of resource usage in two-hop full duplex relay systems based on resource sharing and interference cancellation,” *IEEE Trans. Wireless Commun.*, vol. 8, no. 8, pp. 3933–3938, Aug. 2009.
- [28] T. Riihonen, S. Werner, and R. Wichman, “Mitigation of loopback self-interference in full-duplex MIMO relays,” *IEEE Trans. Signal Process.*, vol. 59, no. 12, pp. 5983–5993, Dec. 2011.
- [29] Z. Zhang, X. Chai, K. Long, A. V. Vasilakos, and L. Hanzo, “Full duplex techniques for 5G networks: self-interference cancellation, protocol design, and relay selection,” *IEEE Commun. Mag.*, vol. 53, no. 5, pp. 128–137, May. 2015.
- [30] Q. Wang, Y. Dong, X. Xu, and X. Tao, “Outage probability of full-duplex AF relaying with processing delay and residual self-interference,” *IEEE Commun. Lett.*, vol. 19, no. 5, pp. 783–786, May. 2015.
- [31] D. P. M. Osorio, E. E. B. Olivo, H. Alves, J. C. S. S. Filho, and M. Latva-aho, “Exploiting the direct link in full-duplex amplify-and-forward relaying networks,” *IEEE Signal Process. Lett.*, vol. 22, no. 10, pp. 1766–1770, Oct. 2015.
- [32] T. Kwon, S. Lim, S. Choi, and D. Hong, “Optimal duplex mode for DF relay in terms of the outage probability,” *IEEE Trans. Veh. Technol.*, vol. 59, no. 7, pp. 3628–3634, Sep. 2010.
- [33] T. Riihonen, S. Werner, and R. Wichman, “Hybrid full-duplex/half-duplex relaying with transmit power adaptation,” *IEEE Trans. Wireless Commun.*, vol. 10, no. 9, pp. 3074–3085, Sep. 2011.
- [34] Z. Zhang, Z. Ma, M. Xiao, Z. Ding, and P. Fan, “Full-duplex device-to-device aided cooperative non-orthogonal multiple access,” *IEEE Trans. Veh. Technol.*, vol. 66, no. 5, pp. 4467–4471, May. 2017.
- [35] I. Krikidis, H. A. Suraweera, P. J. Smith, and C. Yuen, “Full-duplex relay selection for amplify-and-forward cooperative networks,” *IEEE Trans. Wireless Commun.*, vol. 11, no. 12, pp. 4381–4393, Dec. 2012.
- [36] T. M. Cover and J. A. Thomas, *Elements of information theory*, 6th ed., Wiley and Sons, New York, 1991.
- [37] C. Zhong, H. A. Suraweera, G. Zheng, I. Krikidis, and Z. Zhang, “Wireless information and power transfer with full duplex relaying,” *IEEE Trans. Commun.*, vol. 62, no. 10, pp. 3447–3461, Oct. 2014.
- [38] I. S. Gradshteyn and I. M. Ryzhik, *Table of Integrals, Series and Products*, 6th ed. New York, NY, USA: Academic Press, 2000.
- [39] Z. Bai, J. Jia, C. X. Wang, and D. Yuan, “Performance analysis of snr-based incremental hybrid decode-amplify-forward cooperative relaying protocol,” *IEEE Trans. Commun.*, vol. 63, no. 6, pp. 2094–2106, Jun. 2015.